Simulation of Wall Pressure Fluctuations for High Subsonic and Transonic Turbulent Boundary Layers

Nan Hu

German Aerospace Center (DLR), Institute of Aerodynamics and Flow Technology, Department of Technical Acoustic, Email: nan.hu@dlr.de

Introduction

Turbulent boundary layer induced wall pressure fluctuations is one of the major source term for the aircraft cabin noise[1]. Although the features of the wall pressure fluctuations have been extensively studied, most investigations were carried out for incompressible flows. In the present study, wall pressure fluctuations beneath zero pressure gradient turbulent boundary layers are simulated in the high subsonic and transonic flow regimes with Reynolds number on the order of 10 million. The fluctuating pressure within the boundary layer is calculated by solving a Poisson equation. Actually, in a compressible turbulent boundary layer the pressure fluctuations are not governed by the Poisson equation, which holds only for incompressible flow. However, results from experiments[2] carried out in the Transonic-Wind-Tunnel Göttingen and on the Advanced Research Technology Aircraft of the German Aerospace Center[3] show that, the acoustic contribution to the wall pressure fluctuations is negligible compared to the hydrodynamic contribution. Therefore, we are encouraged to compute the pressure fluctuations via the Poisson equation even for the transonic flow, with which the computation can be more efficiently performed. Synthetic turbulence generated with the Fast Random Particle-Mesh Method is used to describe the source terms on the right-hand of the equation. Both the mean-shear term and turbulence-turbulence term are considered. Results are compared to the experimental results carried out in the Transonic-Wind-Tunnel Göttingen.

Numerical Approach

Poisson Equation

Pressure fluctuations within boundary layers are governed by a Poisson equation, reads

$$\Delta p = -\rho_0 \left(2\frac{\partial U_1}{\partial x_2}\frac{\partial u_2}{\partial x_1} + \frac{\partial^2}{\partial x_i \partial x_j}(u_i u_j - \overline{u_i u_j}) \right), \quad (1)$$

where U_1 denotes the mean-flow velocity and u_2 indicates velocity fluctuations in the wall-normal direction; p is the fluctuating pressure and ρ_0 is the mean air density. Note that, the density is variable in a compressible boundary layer flow. The source term on the right-hand side comprises two parts. The first part is the mean-shear term and the second part is the turbulence-turbulence term. If the boundary is a rigid flat surface, the fluctuating pressure can be calculated from the convolution of the free-space Green function of the Poisson equation with the right-hand side source term including the mirror part from the wall, i.e.,

$$p(\mathbf{x},t) = -\int_{\mathbf{V_s}+\mathbf{V_s'}} \rho_0(\mathbf{y}) \left(2\frac{\partial U_1}{\partial x_2}\frac{\partial u_2(\mathbf{y},t)}{\partial x_1} + \frac{\partial^2}{\partial x_i \partial x_j}(u_i u_j - \overline{u_i u_j})(\mathbf{y},t)\right) \cdot g(\mathbf{x}-\mathbf{y})\, d^3\mathbf{y} \quad (2)$$

Here, the integration is carried out over the original source area $\mathbf{V_s}$ plus a source area $\mathbf{V_s'}$ that represents an image of $\mathbf{V_s}$ mirrored at the solid wall. Note that, Eq. (2) is a convolution between the source term and the free-space Green function. The equation can be more efficiently solved in wavenumber domain by using the convolution theorem. For an accurate numerical solution with this approach, a modification as introduced by Hockney and Eastwood[4] is applied, which provides an exact realization of the free-space Green function in conjunction with a Fourier transform method on the finite domain. A detailed description of this approach applied to the Poisson problem can be found in Hu *et al.*[5].

Fast Random Particle-Mesh Method

The synthetic turbulent velocity fluctuations to prescribe the right-hand side source term of Eq. (1) are generated by the Fast Random Particle-Mesh Method (FRPM)[6]. FRPM uses averaged turbulence statistics to synthesize the turbulent velocity fluctuations. One and two-point statistics are realized. The basic idea is to generate a fluctuating vector potential ψ_i with three components from a convolution of spatial white noise $\mathcal{U}_i$ with a spatial Gaussian filter kernel G,

$$\psi_i(\mathbf{x},t) = \int_{\mathbf{V_s}} \hat{A}(\mathbf{x}) G(\mathbf{x}-\mathbf{x}') \mathcal{U}_i(\mathbf{x}',t)\, d^3\mathbf{x}', \quad (3)$$

with

$$G(\mathbf{x}-\mathbf{x}') = \exp\left(-\frac{\pi}{2}\frac{|\mathbf{x}-\mathbf{x}'|}{l_s^2}\right), \quad (4)$$

where $\hat{A}$ denotes an amplitude function whose appropriate scaling yields the desired variance of ψ_i, $\mathbf{x}$ defines field coordinates of the vector potential and $\mathbf{x}'$ defines white noise field coordinates. Furthermore, l_s is an integral turbulent length scale determined from the Reynolds averaged Navier-Stokes (RANS) calculation,

$$l_s^* = \frac{c_l}{C_\mu}\frac{\sqrt{k_t^*}}{\omega^*}, \quad (5)$$

where $k_t^* = k_t/U_{ref}^2$ is the turbulent kinetic energy and $\omega^* = \omega \cdot l_{ref}/U_{ref}$ is the specific rate of dissipation. The

expression $*$ denotes non-dimensional parameters. The reference quantities are set l_{ref} to 1 m and U_{ref} to the sound speed. The constant $C_\mu = 0.09$ and c_l is estimated to be 0.54[7], so the pre-factor $c_l/C_\mu \simeq 6.0$. An anisotropy of the length scale can be realized by applying a stretching factor γ. It is assumed that the relationship $l_s = (l_1 l_2 l_3)^{1/3}$ and $1/\gamma \cdot l_1 = l_2 = l_3$. In the present calculation, γ is chosen to be 1.5 according to Hu *et al.*[5].

The fluctuating velocities can be obtained by taking the curl of the fluctuating potential field $\boldsymbol{\psi}$,

$$u_i = \epsilon_{ijk} \frac{\partial \psi_k}{\partial x_j}. \tag{6}$$

For sufficiently slow spatially changing length scale l_s and amplitude $\hat{A}$ the derivatives of ψ_i can be expressed through analytical derivatives of the Gaussian filter kernel,

$$u_i(\mathbf{x}, t) = \int_{\mathbf{V_s}} \hat{A}(\mathbf{x}) \epsilon_{ijk} \frac{\partial G(\mathbf{x} - \mathbf{x}')}{\partial x_j} \mathcal{U}_k(\mathbf{x}', t)\, d^3\mathbf{x}'. \tag{7}$$

The white noise field $\mathcal{U}_i$ is defined in a Lagrangian frame moving at local flow velocity $\mathbf{U}$. Additional temporal turbulence decay can be modeled by a Langevin equation, which introduces the decorrelation in the two-points statistics[6]. Altogether, the cross-correlation properties of the white noise is given by

$$< \mathcal{U}_i(\mathbf{x}', t) \mathcal{U}_j(\mathbf{x}' + \mathbf{r}, t+\tau) >= \delta(\mathbf{r} - \mathbf{U}\tau) \exp\left(-\frac{|\tau|}{\tau_s}\right) \delta_{ij}, \tag{8}$$

where the bracket means an ensemble average, δ_{ij} is the Kronecker symbol, $\delta(\mathbf{r} - \mathbf{U}\tau)$ describes a frozen turbulence flow moving with the flow velocity $\mathbf{U}$ and $\exp(-|\tau|/\tau_s)$ involves the turbulence decay, i.e. the spatially white noise is correlated in time with time-scale τ_s. The local time scale is determined from RANS calculations,

$$\tau_s^* = C_\tau \frac{l_s^*}{\sqrt{k_t^*}}. \tag{9}$$

The pre-factor $C_\tau = 1.2$ is applied herein according to Hu *et al.*[5].

The Reynolds stress anisotropy can be obtained using a scaling tensor, which is deduced by the relationship between the anisotropic Reynolds stress provided by RANS calculations and the isotropic Reynolds stress tensors.

For more details about the FRPM implementation in computational domain and properties of the generated synthetic turbulence refer to the work of[6], and about the approach of turbulence anisotropy refer to Hu *et al.*[5].

Computational Setups

Mean flow statistics for two-dimensional flat plate boundary layers are obtained from RANS calculations using DLR's CFD code TAU. A high subsonic flow Ma=0.57 and a transonic flow Ma=0.83 are calculated. The

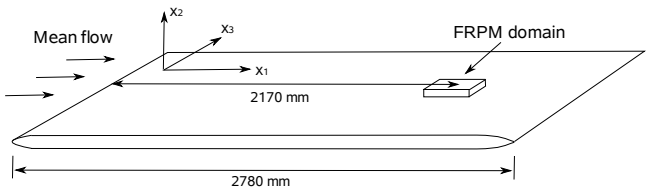

Figure 1: Sketch of the computational domain.

Ma	δ (mm)	δ^* (mm)	θ (mm)	H δ^*/θ	Re_x $U_0 L_x/\nu$	Re_τ $u_\tau \delta/\nu$
0.57	26.8	4.36	3.02	1.45	$10.4{\cdot}10^6$	4502
0.83	26.6	4.58	2.86	1.60	$11.5{\cdot}10^6$	4933

Table 1: Turbulent boundary layer parameters.

Reynolds stress model with specific dissipation (ω) is used for the calculation. The boundary layer is solved on a structured grid with about 200K mesh points and the first cell layer $y^+ < 1$.

A sketch of the computational domain is shown in Fig. 1. Synthetic turbulence is realized by FRPM for a three-dimensional rectangular domain with its center located 2.17 m downstream of the leading edge. The extension of the FRPM domain is $L_1 = 6\delta$, $L_2 = 1.2\delta$ and $L_3 = 3\delta$ in streamwise, wall-normal and spanwsie direction, respectively, where δ denotes the boundary layer thickness at the center of the domain. Since Hockney's method demands for a grid with 2^N mesh points in each direction, a cartesian grid with $128 \times 64 \times 64$ points is used for the calculations. The calculations are computed on 4 Inter Xeon E5-2630 2.4GHz CPUs (8 threads) and for 0.5s real time for each case. For Ma=0.57 the calculation time is about 8 days and for Ma=0.83 11 days due to a smaller time step needed.

Table 1 shows the gained boundary layer parameters from RANS solutions. The boundary layer parameters for the computational domain were not provided from the experiment. The boundary layer thickness was measured by pressure tubes at $x = 1645$ mm for an wedge-shaped trailing edge configuration in a previous test and was es-

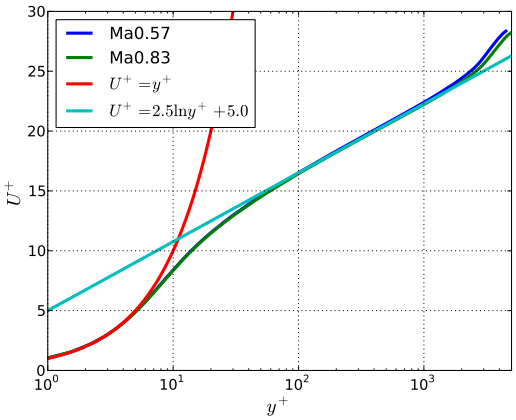

Figure 2: Boundary layer mean velocity profile.

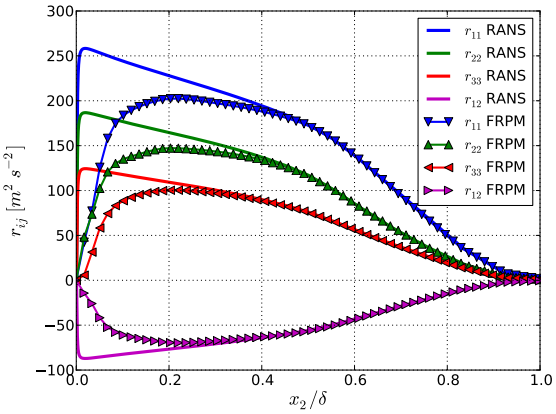

Figure 3: Reconstruction of Reynolds stress tensors.

timated about 24 mm. Fig. 2 shows the boundary layer mean velocity profiles for both velocities, which present the typical zero pressure gradient boundary layer profiles. Interesting is that the shape factor H is 1.45 for Ma=0.57 and 1.6 for Ma=0.83, whose values relate to adverse pressure gradient boundary layer mean velocity profiles. The reason for that is the density is smaller in the region closer to wall due to the temperature increase towards wall for a compressible boundary layer flow.

Results

Reynolds stress Realization

Turbulence velocity fluctuations realized by FRPM are used to prescribe the fluctuating source terms of the Poisson equation (1). To verify a proper realization of the fluctuating velocity from FRPM, Fig. 3 shows the reconstructed Reynolds stress tensors for Ma=0.83 in comparison to the tensors gained from RANS within the boundary layer. A very good reconstruction of the tensors is found in the outer region $> 0.3\delta$. A attenuation of the level is visible in the region $< 0.3\delta$, especially for $< 0.1\delta$, which mainly because the used grid resolution is not fine enough to resolve the small turbulence structures close to the wall.

One-point Spectra

The pressure fluctuations are computed according to Eq. (2) using integration by parts. The mean-shear term p_{ms} and the turbulence-turbulence term p_{tt} are separately solved. Thus, the sum of the two parts results the total pressure fluctuations p_{total}.

Fig. 4 shows the calculated wall pressure spectra of p_{ms}, p_{tt} and p_{all} for both velocities. The contributions of p_{ms} and p_{tt} are in the same order, which agrees with the DNS/LES results from Kim[8] and Chang *et al.*[9] for channel flow at low Reynolds numbers. The spectra of p_{ms} increase at low frequencies and drops after reaching a maximum at medium frequencies, whereas p_{tt} show a low-frequency plateau. Those trends of both contributions make p_{tt} dominates the low frequencies and p_{ms} takeovers the roll from mid-frequencies. Both p_{ms} and p_{tt}

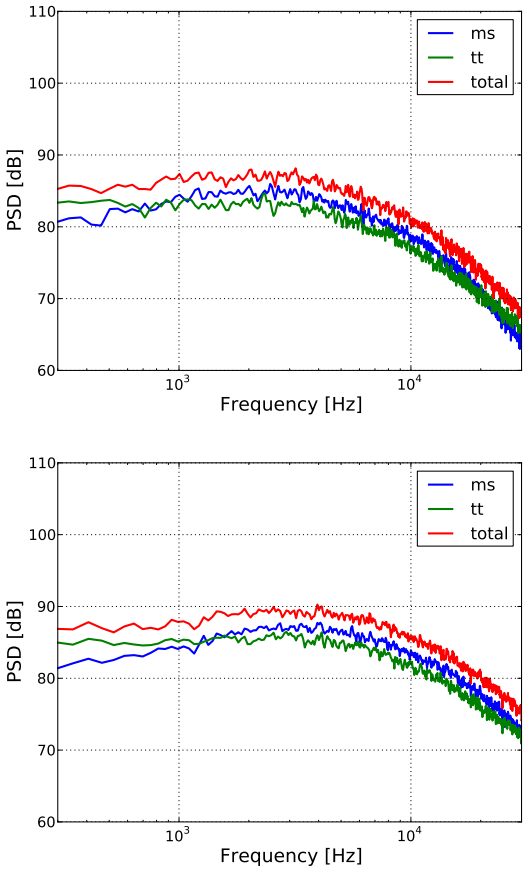

Figure 4: Numerical results for the wall pressure spectra. (up), Ma=0.57; (down), Ma=0.83.

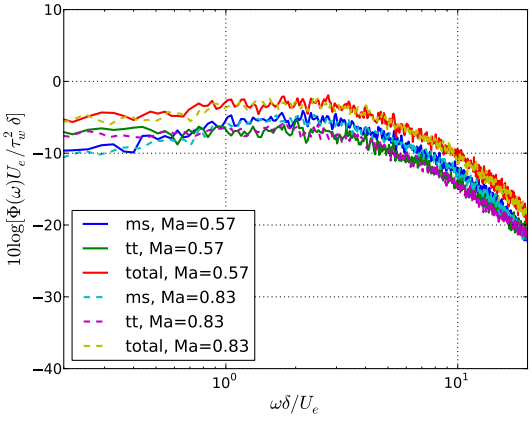

Figure 5: Numerical results scaled with scaled by $U_e/\tau_w^2\delta$ as pressure scale and δ/U_e as time scale.

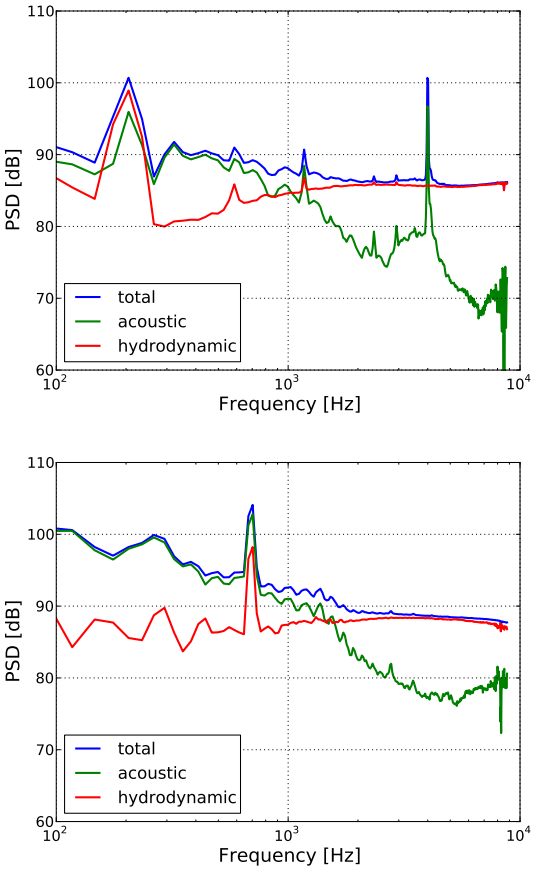

Figure 6: Experimental results for the wall pressure spectra. (up), Ma=0.57; (down), Ma=0.84.

and therefore the p_{total} scale well with $U_e/\tau_w^2\delta$ as pressure scale and δ/U_e as time scale, see Fig. 5.

Fig. 6 shows the experimental results provided by Ehrenfried[2]. The pressure fluctuations were measured using an array of 48 miniature piezo-resistive pressure sensors. Through the beamforming technique, the acoustic part can be separated from the hydrodynamic part till about 9 kHz due to the limitation of the used array. The results show that the measured spectra are contaminated by the wind tunnel noise at low frequencies. At medium frequencies the measured acoustic noise, which is assumed that contributed from the turbulent boundary layer noise and the trailing edge noise, is negligible, about 10 dB smaller than the hydrodynamic pressure fluctuations at Ma=0.84. The dominance of the hydrodynamic pressure fluctuations compared to the acoustic noise is assumed to be true also for low frequencies if only the turbulent boundary layer noise is considered.

The numerical results are compared to the measured hydrodynamic pressure fluctuations, shown in Fig. 7. The gained hydrodynamic at low frequencies where the signal (total) to noise (acoustic) ratio less than 1 dB is not considered. Note that, the Helmholtz resonance was excited in the cavity of the pinhole-mounted sensors for Ma=0.57 at about 10 kHz. The impact of the resonance on the spectrum can be found down to about 5 kHz. Thus, the spectrum above 5 kHz for Ma=0.57 is not considered.

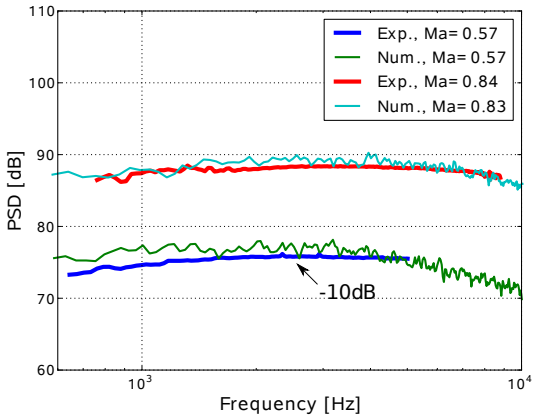

Figure 7: Comparison of the wall pressure spectra between experimental and numerical results.

Furthermore, the peaks in the spectra are smoothed. The calculated spectra p_{total} for both velocities show excellent agreement with the measured results. Consequently, we may draw the conclusion that for a compressible flow as long as the acoustic pressure fluctuations in comparison to the hydrodanamic fluctuations can be neglected, the wall pressure fluctuations can be well determined via the Poisson equation.

References

[1] Hu, N.: Contributions of Different Aeroacoustic Sources to Aircraft Cabin Noise, AIAA paper, 2013

[2] Ehrenfried, K. and Koop, L.: Experimental study of pressure fluctuations beneath a compressible turbulent boundary layer. AIAA Paper, 2008

[3] Haxter, S. and Spehr, C.: In-Flight Determination of Acoustic and Hydrodynamic Pressure Fluctuations. DAGA, 2013

[4] Hockney, R. W. and Eastwood, J. W.: Computer simulation using particles, Taylor & Francis, Inc., 1988.

[5] Hu, N., Reiche, N. and Ewert, R.: Simulation of turbulent boundary layer wall pressure fluctuations via Poission equation and synthetic turbulence. (submitted to J. Fluid Mech., 2016)

[6] Ewert, R., Dierke, J., Siebert, J., Neifeld, A., Appel, C., Siefert, M., and Kornow, O.: CAA broadband noise prediction for aeroacoustic design. J. Sound Vib., Vol. 330, 2011.

[7] Bailly, C. and Juvé, D.: A stochastic approach to compute subsonic noise using linearized Euler's equations. AIAA Paper, 1999

[8] Kim, J.: On the structure of pressure fluctuations in simulated turbulent channel flow. J. Fluid Mech., Vol. 205, 1989

[9] Chang, P. A., Piomelli, U. and Blake, W. K.: Relationship between all pressure and velocity-field sources. Phys. Fluids, Vol. 11, 1999